

Heat Transfer Enhancement in a Baffled Attic-Shaped Space

Suvash C. Saha, Y.T. Gu and M.M.K. Khan

Abstract To reduce the natural convection heat loss from attic-shaped spaces, many researchers used convection suppression devices in the past. In this chapter, a single baffle is used under the top tip to investigate numerically the natural convection heat loss in an attic-shaped enclosure, which is a cost-effective approach. The case considered in this chapter is one inclined wall of the enclosure which is uniformly heated while the other inclined wall uniformly cooled with adiabatic bottom wall. The finite volume method has been used to discretize the governing equations, with the QUICK scheme approximating the advection term. The diffusion terms are discretized using central differencing with second-order accuracy. A wide range of governing parameters is studied (Rayleigh number, aspect ratio, baffle length, etc.). It is observed that the heat transfer due to natural convection in the enclosure reduces when the baffle length is increased. Effects of other parameters on heat transfer and flow field are described in this study.

1 Introduction

One of the most important forms of heat transfer and fluid flow in an enclosure is natural convection where the fluid motion is simply induced by density gradients due to temperature differences. Natural convection in enclosures has received extensive attention during past few decades due to its superior importance and applications in nature and industry. Various cavities and spaces such as rectangular shapes, annular spaces, and cylindrical cavities subjected to different thermal and moving boundary conditions have been investigated employing useful working

S.C. Saha (✉) · Y.T. Gu

School of Chemistry, Physics and Mechanical Engineering, Queensland University of Technology, GPO Box 2434, Brisbane, QLD 4001, Australia
e-mail: suvash.saha@qut.edu.au; s_c_saha@yahoo.com

M.M.K. Khan

School of Engineering & Built Environment, Central Queensland University, Rockhampton Campus, Rockhampton, QLD 4702, Australia

© Springer Nature Singapore Pte Ltd. 2018

M.M.K. Khan et al. (eds.), *Application of Thermo-fluid Processes in Energy Systems*, Green Energy and Technology, https://doi.org/10.1007/978-981-10-0697-5_7

fluids such as water and air. The comprehensive review and discussion about the researched topics can be found in [1–4]. However, it is important to note that models attributed to rectangular cavities cannot estimate the complete buoyancy-driven flow within geometries with variable or sloping boundaries. Even though natural convection in a triangular enclosure [5] has many engineering applications in energy transfer in rooms and buildings, convective motion in solar stills, nuclear reactor cooling, and electronic equipment cooling it receives much less attention.

Attic-shaped buildings expose to different thermal boundary conditions during a daytime dependent on the climate situation. Therefore, the natural convection process within the space should be precisely revealed. Since the thermal and fluid flow conditions should provide comfort for the present people according to residential ventilation standards, the space geometry, inside structure, and the insulation are important factors for better design. Moreover, energy consumption for air-conditioning should be considered to achieve higher energy efficient building. According to those literature attended for natural convection within enclosures, fluid flow and heat transfer phenomena are limited for triangular spaces.

One of the earliest studies on natural convection in triangular cross-sectional enclosure was conducted by Probert and Thirst [6, 7]. In their experiment studies, the authors found the optimal pitch angle leading to the minimum rate of heat transfer in the attic of a modeled pitched roof with specified boundary conditions. They showed that the contribution by convection heat transfer is increased rather than conduction with the increase of aspect ratio up to a critical value.

Flack [8, 9] performed several experimental tests using isosceles triangular enclosure filled with air for various aspect ratios and Rayleigh numbers. The enclosure was cooled or heated from base boundary and heated or cooled from inclined walls. Thermal and fluid flow pattern was investigated as well as local and average Nusselt number of heated or cooled walls. It was found that for the case of base heating and inclined cooling, with the increase of Rayleigh number, laminar free convection heat transfer regime became unstable achieving to a critical Rayleigh number, where flow pattern altered to turbulent natural convection regime. Latter, natural convection in a right-angled triangular enclosure with bottom heating and cold side walls for air and distilled water was studied by Poulikakos and Bejan [10, 11] where Rayleigh–Benard type convection occurred. The authors established a new relationship for mean Nusselt number when air filled the enclosure. Considering similar boundary conditions proposed by Flack [5, 6] for their experimental works, Ridouane et al. [12] numerically found a good agreement after comparison of Nusselt number. Latter, Ridouane et al. [13] cut both bottom tips off significantly with exposing thermal insulation boundary condition and reported a much energy efficient space, which consumes less energy to keep the region at desired temperature. There are several studies conducted to deal with the stability of flow cellular structure [14–17]. In their studies, they reported the flow pattern for

different boundary conditions with emphasis on the stability of the single cell formed at the core of the region followed by cell division into several smaller pieces and found out some transitional conditions with respect to the aspect ratio and Rayleigh number.

Holtzman et al. [18] performed series of experiments using smoke injected into the triangular enclosure with bottom heated and cold side inclined walls. Symmetry flow assumption was reported for lower Rayleigh number; however, with the increase of Rayleigh number first time they observed asymmetry and multicellular flow progressed inside the enclosure denoting the appearance of pitchfork bifurcation. Predictions of symmetry bifurcation of buoyancy-driven flow within triangular cavity numerically were studied again by Ridouane and Campo [19]. Their numerical reports indicated a critical Rayleigh number of 1.42×10^5 in which for Ra above that critical value, subcritical pitchfork bifurcation is created. The appearance of pitchfork bifurcation is also investigated for diurnal thermal forcing condition [20] where the temperature on inclined surfaces sinusoidally changes with time.

Recently, fluid flow and heat transfer inside an attic space for the boundary conditions of sudden heating/cooling and ramp heating/cooling have been analyzed by Saha et al. [21–24] by employing scaling analysis with numerical verifications. The authors studied the transient flow development inside the enclosure and showed different stages of the flow development.

Since one of the main objectives of designing a residential house is to reduce the heat transfer inside the attic space, several researchers have conducted research by adding adiabatic fin on the walls [25–29]. Varol [25] incorporated single thin adiabatic plate onto a triangular cavity in order to disrupt the heat flow. It was found that for a low Rayleigh number, the main mode of heat transfer is by conduction which is in line with the definition of Rayleigh number. From this research, the maximum and minimum mass flow of the stream function can be decreased by increasing the distance of the plate from the origin. For better understanding on the way of affecting heat transfer in a triangular enclosure, more works have been conducted by adding adiabatic fins on several places of the walls [26]. This is similar to a study conducted by Chamkha [27] with the addition of a single fin to the base of the triangle.

In this chapter, we will focus on a numerical investigation of the steady natural convection in a triangular enclosure with a baffle attached to the top tip. The finite volume method has been used to solve the governing equations. Effects of Rayleigh number, aspect ratio, and baffle length on heat transfer and flow field are described in this study. It is found that the effect of the length of the baffle or interrupter has a great influence on the heat transfer. The results are presented as a form of temperature contours and stream functions. The heat transfer is represented as a form of Nusselt number.

2 Model Theory

Natural convection in an attic space satisfies the conservation equations of mass, momentum, and energy under the assumption of continuous media. The mathematical expressions of these conservation equations may be written together with the equation of state in Cartesian tensor notations as follows.

The equation for conservation of mass, or continuity equation,

$$\frac{\partial \rho}{\partial t} + \frac{\partial(\rho u_j)}{\partial x_j} = 0, \quad (1)$$

where t is the time, ρ is the density of the fluid, u_j are the velocity components, and x_j are the Cartesian coordinates. Conservation of momentum based on Newton's second law,

$$\rho \frac{Du_i}{Dt} = \frac{\partial \rho}{\partial x_i} + \rho F_i + \frac{\partial}{\partial x_j} \left[\mu \left(\frac{\partial u_i}{\partial x_j} + \frac{\partial u_j}{\partial x_i} \right) \right] - \frac{2}{3} \frac{\partial}{\partial x_i} \left(\mu \frac{\partial u_j}{\partial x_j} \right), \quad (2)$$

where p is the pressure, F_i are body forces, and μ is the viscosity. The conservation of energy equation is:

$$\rho c_p \frac{DT}{Dt} = u_j \frac{\partial \rho}{\partial x_i} + \frac{\partial}{\partial x_j} \left(k \frac{\partial T}{\partial x_j} \right) + \mu \left[\frac{\partial u_j}{\partial x_j} \left(\frac{\partial u_i}{\partial x_j} + \frac{\partial u_j}{\partial x_i} \right) - \frac{2}{3} \left(\frac{\partial u_j}{\partial x_j} \right)^2 \right], \quad (3)$$

where T is the temperature, c_p is specific heat, and κ is the thermal diffusivity. The equation of state is:

$$\rho = \rho(p, T), \quad (4)$$

In Eq. (2), the body force F_i has three components: F_x , F_y , and F_z in x -, y -, and z -directions, respectively. In addition, D/Dt is a derivative operator defined as,

$$\frac{D}{Dt} = \frac{\partial}{\partial t} + u_j \frac{\partial}{\partial x_j}, \quad (5)$$

3 Appropriate Assumptions

The governing Eqs. (1)–(3) are general forms of conservation equations and may be simplified for particular problems such as the one considered in this chapter. Moreover, these equations are highly nonlinear and coupled and are very difficult to solve. Therefore, it is of significance to simplify these equations based on particular

features such as follows so that numerical discretization and analyses can be easily performed.

For the steady natural convection through the inclined wall of an attic space, it is understood that, when heat is added to the fluid, the fluid expands and thus changes its density. If the gravity is present, this change in density induces a change in the body force, which may cause the fluid to move by itself without any externally imposed flow velocity. If the temperature difference between the walls and the ambient is not very large, the correlation between the density and the temperature may be considered as a linear relation. As a result, the equation of state (4) may be given by

$$\rho = \rho_0[1 - \beta(T - T_0)], \tag{6}$$

where β is the thermal expansion coefficient. It is generally of an order of magnitude between 10^{-2} and 10^{-4} for different fluids [30].

The natural convection flows often involve a relatively small temperature difference and a low flow velocity, and thus, an incompressible flow assumption is appropriate (see [31]). Accordingly, the continuity equation (1) may be simplified as follows,

$$\frac{\partial u_j}{\partial x_j} = 0. \tag{7}$$

The Boussinesq approximation is assumed for this problem, meaning that all fluid properties such as the viscosity and the thermal conductivity are treated as constants except the density in the buoyancy term. In the present study, a two-dimensional coordinate system has been adopted, where the x -axis and the y -axis are parallel to the horizontal and the vertical, respectively (see Fig. 1). The effect of the gravitational acceleration on the flow field is along the y -axis. Since there is no other volumetric force, the body force in Eq. (2) may be written as

$$\rho F = -g(\rho - \rho_0). \tag{8}$$

Substituting Eq. (6) in Eq. (8) and applying the Boussinesq approximation, we have

$$F = -g\beta(T - T_0) \tag{9}$$

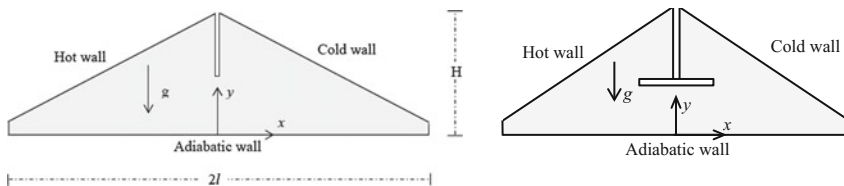


Fig. 1 Schematic of the geometry and the boundary conditions

Now Eq. (2) becomes after incorporating Eqs. (7), (8), and (9)

$$\frac{Du_i}{Dt} = -\frac{1}{\rho} \frac{\partial p}{\partial x_i} + \nu \frac{\partial^2 u_i}{\partial x_j \partial x_j} \pm Fx_i. \quad (10)$$

Similarly, the energy equation can be simplified by assuming that the viscous energy dissipation and the pressure gradient associated with the incompressible assumption may be neglected if the velocity induced by the natural convection flow is lower. Therefore, the energy equation (3) can be simplified as

$$\frac{DT}{Dt} = k \frac{\partial^2 T}{\partial x_j \partial x_j}. \quad (11)$$

The simplified and normalized steady continuity, momentum, and energy equations of a 2D model are expressed as follows:

$$\frac{\partial u}{\partial x} + \frac{\partial v}{\partial y} = 0, \quad (12)$$

$$u \frac{\partial u}{\partial x} + v \frac{\partial u}{\partial y} = -\frac{1}{\rho} \frac{\partial p}{\partial x} + \text{Pr} \left(\frac{\partial^2 u}{\partial x^2} + \frac{\partial^2 u}{\partial y^2} \right), \quad (13)$$

$$u \frac{\partial v}{\partial x} + v \frac{\partial v}{\partial y} = -\frac{1}{\rho} \frac{\partial p}{\partial y} + \text{Pr} \left(\frac{\partial^2 v}{\partial x^2} + \frac{\partial^2 v}{\partial y^2} \right) + \text{Ra Pr } T, \quad (14)$$

$$u \frac{\partial T}{\partial x} + v \frac{\partial T}{\partial y} = \frac{\partial^2 T}{\partial x^2} + \frac{\partial^2 T}{\partial y^2}. \quad (15)$$

The above set of governing equations has been successfully adopted in previous numerical simulations of natural convection in cavity (see, e.g., [32, 33]). It is noted that in the case with a large temperature difference, the fluid does not satisfy the Boussinesq approximation, and thus, cautions must be taken when adopting the above equations.

The Rayleigh number, Ra and the Prandtl number, Pr are defined by

$$\text{Ra} = \frac{g\beta\Delta TH^3}{\kappa\nu} \text{ and } \text{Pr} = \frac{\nu}{\kappa}, \quad (16)$$

where ν is the kinematic viscosity.

The aspect ratio and the Nusselt number are defined as

$$A = \frac{H}{l} \text{ and } \text{Nu} = \frac{qH}{\Delta Tk}, \quad (17)$$

where q is the convective heat flux through a boundary and k is the thermal conductivity.

4 Problem Description

Under consideration is the steady flow behavior resulting from heating/cooling a quiescent, isothermal Newtonian fluid of air in a two-dimensional triangular enclosure of height H and horizontal length $2l$ (see Fig. 1). There is a flow interrupter (baffle) attached with the top tip of the enclosure. The baffle with or without a blade attached at the end will affect the flow field. The left inclined surface is heated and the right inclined surface is cooled, whereas the bottom base and the sides of the baffle and the blade are adiabatic as shown in Fig. 1. All boundaries are considered as nonslip. It is also assumed that the flow is laminar. In order to avoid the singularities at the tips in the numerical simulation, the tips are cut off by 5% and at the cutting points (refer to Fig. 1) rigid nonslip and adiabatic vertical walls are assumed. We anticipate that this modification of the geometry will not alter the overall flow development significantly [20, 21].

The initial and boundary conditions are defined as follows:

- Initially, the fluid is quiescent and isothermal.
- On the sloping walls, a rigid nonslip and uniform heating temperature conditions are applied on the left wall and uniform cooling temperature conditions are applied on the right wall (see Fig. 1).
- The bottom horizontal wall, sides of the baffle and blade are maintained as adiabatic and rigid nonslip.
- At the cutting points of the bottom tips, rigid nonslip and adiabatic vertical walls are assumed.

The governing equations (1)–(4) along with the specified initial and boundary conditions are solved using control volume method. The finite volume scheme has been chosen to discretize the governing equations, with the QUICK scheme approximating the advection term. The diffusion terms are discretized using central differencing with second-order accuracy. An extensive grid independence test has been carried out for this study. The results are not shown here for brevity. The suitable numbers of grid nodes adopted for three different aspect ratios of $A = 1.0$, 0.5 , and 0.2 are 169×848 , 166×744 , and 160×532 , respectively.

5 Results and Discussions

Results are presented in the form of isotherms and stream functions as well as Nusselt number in this study. Effects of Rayleigh number, aspect ratio, baffle height, and blade length on heat transfer and fluid flow have been presented and discussed in details.

5.1 Effects of Length of the Interrupter

Temperature contours and the stream functions are shown in Fig. 2. It is clearly observed that with the addition of an interrupter on the top tip of the enclosure, the heat transfer within the enclosure changes drastically. Due to buoyancy effect, the hot air should travel along the left inclined wall and when it reaches the top tip the thermal stratification starts to happen. As the length of the interrupter increases, the

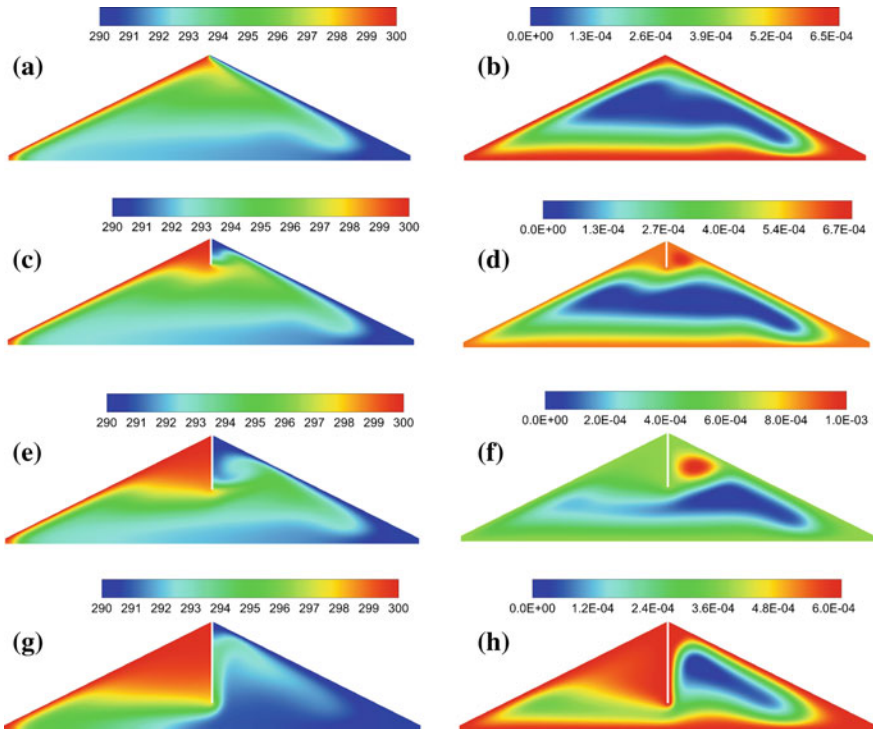


Fig. 2 Temperature contours (*left*) and stream functions (*right*) for different length of the interrupter; **a, b** no interrupter, **c, d** 25% of H , **e, f** 50% of H , **g, h** 75% of H when $Ra = 10^6$ and $A = 0.5$

heat trapped on the hot side of the wall increases. This is due to the nature of heated air which does not flow downward easily due to buoyancy. This is clearly seen in the enclosure for the case when the length of the interrupter is 75% of the cavity height. The buildup of heat layers occurs before the heat begins to flow to the cold wall. This modification of the geometry would be very beneficial during winter conditions as the trapped layer of heated air would play a vital role in heating the house and have a significant saving in heating application.

5.2 Effect of Rayleigh Numbers

Figure 3 represents the temperature contours and stream functions for different values of Rayleigh number. It is observed from this figure that for low Rayleigh number single cell is visible; however, as Rayleigh number increases, the solution becomes a two-vortex solution and with further increase in the Rayleigh number a multiple vortex solutions can be observed. It is also observed from the temperature contours that the thermal boundary layer for low Rayleigh number is thicker. However, with increase of Rayleigh number the thermal boundary layer becomes thinner (concentrated near the inclined walls). That means, the flow is dominated by convection.

Effect of Rayleigh number on fluid flow and heat transfer is shown for two Rayleigh numbers in the presence of a blade attached horizontally to the baffle end

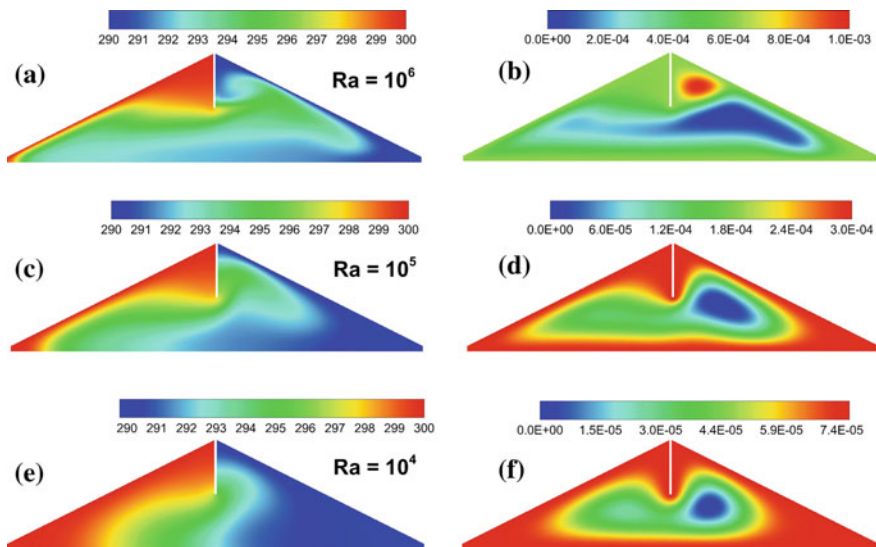


Fig. 3 Temperature contours (*left*) and stream functions (*right*) for different Ra while $A = 0.5$ and length of the interrupter is 50% of height

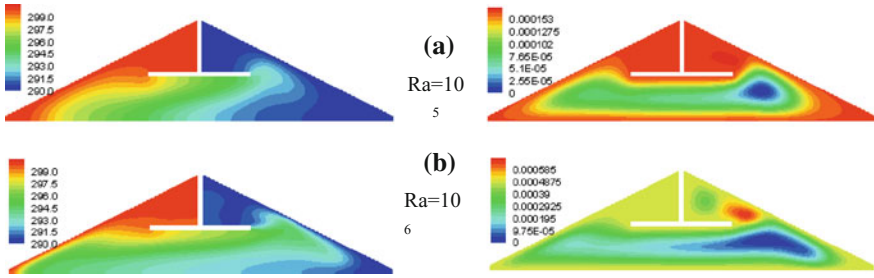


Fig. 4 Temperature contours (*left*) and stream functions (*right*) for different Ra while $A = 0.5$ and length of the interrupter is 50% of height

in Fig. 4. It is observed that the air flow is severely affected by the presence of horizontal blade. As Rayleigh number increases, the flow becomes stronger due to convection dominates the flow. The hot fluid travels underneath the blade and tries to cover the right side of the baffle. We have also observed multicellular flow structure as Ra increases.

5.3 Effects of Aspect Ratio

To show the effect of aspect ratio (height to base ratio), temperature contours (a, c, e) and the stream functions (b, d, f) are depicted in Fig. 5. Three aspect ratios have been considered as $A = 1.0, 0.5,$ and 0.2 .

From the temperature contour in Fig. 5, it is observed that the heat distribution is the quickest when the aspect ratio is the lowest whereas heat distribution is the lowest when the aspect ratio is the highest. These phenomena can be verified by the stream function. For the aspect ratio of 0.2 , there are areas of concentrated lines indicating a low pressure, high-velocity zone. With this low pressure, it would act as a vacuum to ensure air distribution from the left side of the enclosure to the right side. However, for the aspect ratio of 1.0 , there are larger pockets of cooler air compared to the 0.2 ratio. This is due to the heat being trapped in the upper areas of the enclosure.

5.4 Effect of Blade Length

The effect of blade length on fluid flow and heat transfer is presented in Fig. 6. It is observed that when the blade is longer the hot fluid from the left side of the enclosure travels through the underneath of the horizontal blade. It does not get much space to travel to the top right side of the enclosure. This region is controlled

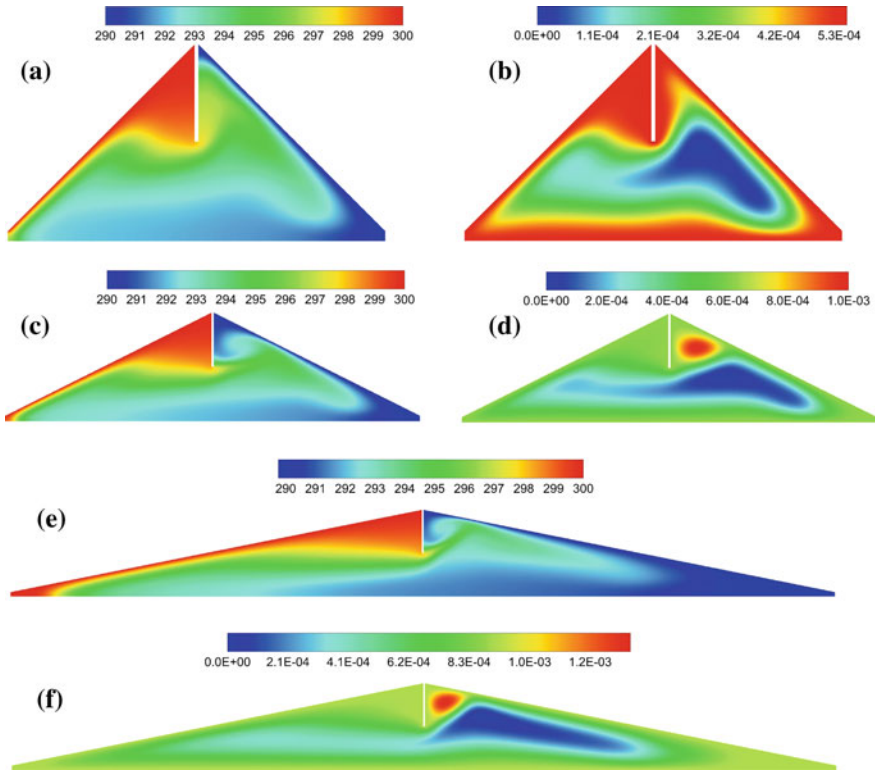


Fig. 5 Temperature contours (a, c, e) and stream functions (b, d, f) for different A while $Ra = 10^6$ and length of the interrupter is 50% of height

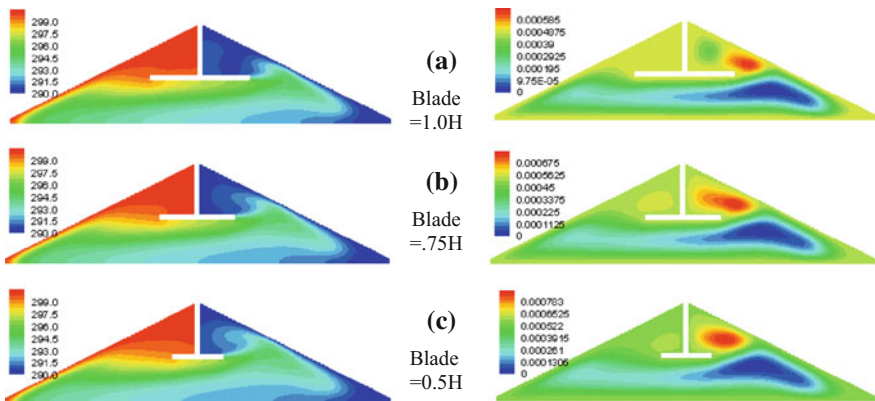


Fig. 6 Temperature contours (left) and stream functions (right) for different Ra while $A = 0.5$ and length of the interrupter is 50% of height

by cold fluid. However, as the blade length decreases the hot fluid gets much space to enter the top right region. We also observed multicellular regions in the stream function.

5.5 Heat Transfer

Figure 7 shows the Nusselt number calculated on the inclined surfaces of the enclosure. Figure 7a represents variation of Nu for variation of the length of the interrupter. It is found that when there is no interrupter the heat transfer through the inclined walls is the highest. However, the heat transfer becomes lower when the length of the interrupter increases. The lowest Nusselt number calculated is for

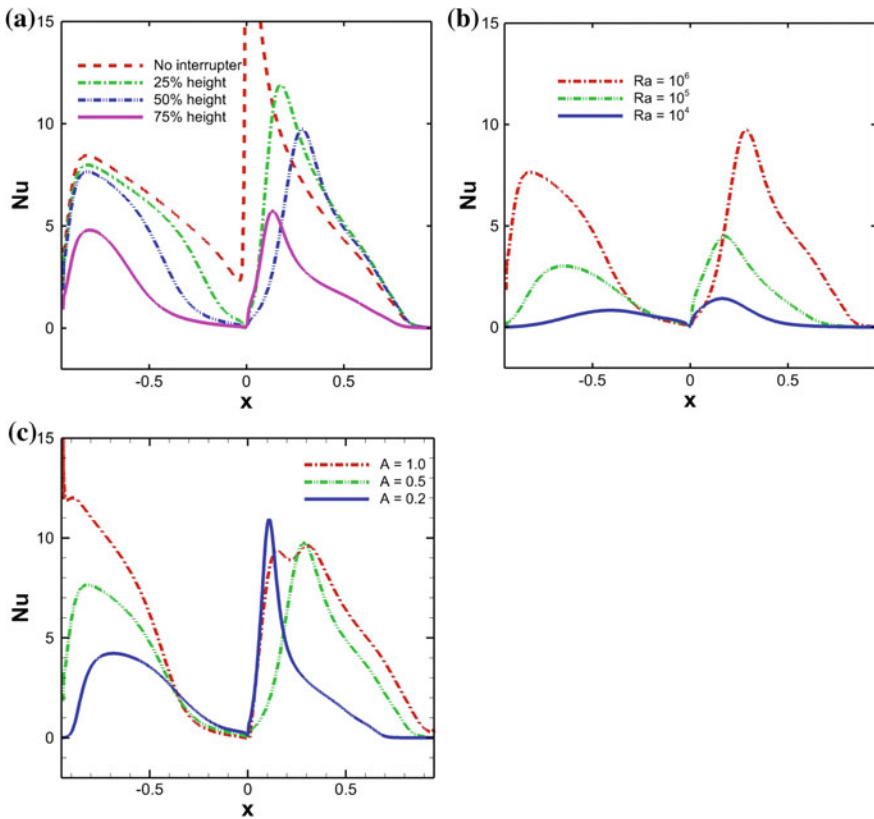


Fig. 7 Nusselt number calculated on the inclined surfaces: **a** effect of interruption for $Ra = 10^6$ and $A = 0.5$, **b** effect of Ra when $A = 0.5$ and length of interrupter is 50% of H , and **c** effect of A while $Ra = 10^6$ and length of interrupter is 50% of H

75% of the height of the enclosure which is the highest length of the interrupter. In Fig. 5b, the heat transfer is higher for higher Rayleigh number which is expected due to the fact that convection dominates the heat transfer for higher Rayleigh number. Variation of Nu is shown for different aspect ratios and is shown in Fig. 5c. It is found that heat transfer is lower for lower aspect ratio. Since the base of the enclosure is much longer than its height, the heat transfer near the two tips (left and right tips) is dominated by conduction. The mixing of hot and cold air occurs quicker.

Nusselt number is also calculated on the inclined walls for different values of blade length. It is observed that when the blade length is smaller the heat transfer rate is higher on the left inclined wall. As the blade length increases, the heat transfer decreases as the hot fluid from the left side of the enclosure does not get much space to travel to the right top region. The heat transfer through the right inclined wall is bit complex. However, for lower value of blade length, the heat transfer is the highest. When the length of the blade is similar to the interrupter height the heat transfer is the highest near $x = 0.9$. This is because the hot fluid from the left side of the enclosure travels through the underneath of the blade and hits the right inclined wall near $x = 0.9$. Near the top tip, the heat transfer is lower. Therefore, it can be concluded that in the presence of baffle attached to the top tip causes heat transfer reduction through the inclined walls of the enclosure. Heat transfer is also reduced when the baffle height increases or the blade length increases (Fig. 8).

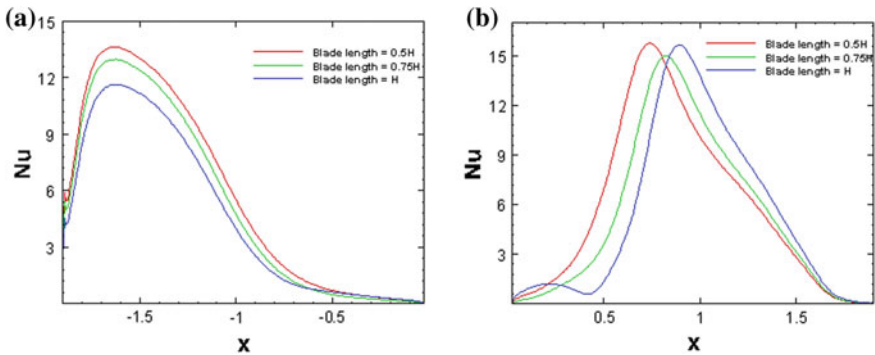


Fig. 8 Nusselt number calculated on the **a** left and the **b** right inclined surfaces for different blade length for baffle height = 0.5, $Ra = 10^6$, and $A = 0.5$

6 Conclusions

This study shows the enhancement/suppression of natural convection when there is a modification of the geometry, i.e., the aspect ratio, or addition of an interrupter hanging vertically from the apex of the triangular enclosure. From the simulations obtained, it is found that with the addition of an interrupter, the heat transfer is significantly reduced. It is also found that the heat transfer reduces as the height of the interrupter increases. This would be a useful application on houses with winter climates. The trapped heat would be able to heat the interior of the house reducing the power consumption for heating devices. Here, it has also been demonstrated that with a higher aspect ratio, the mass transfer of the air decreases while with a lower aspect ratio the mass transfer increases, thereby increasing the flow and mixing of hot air with the cold air.

For further studies on the effects of an interrupter on the heat flow in an attic space, the geometry of the interrupter has been modified. A horizontal adiabatic blade is attached at the end of the baffle. Inclusion of this blade further reduces the heat transfer. Moreover, the heat transfer depends on the length of the blade. When the blade length is smaller, the heat transfer is higher. However, as the length of the blade increases the heat transfer decreases. To ensure that the interrupter would be viable for both summer and winter conditions, it would be recommended to introduce movable covered slots onto the interrupter itself. The purpose of these slots is to allow heat flow through the interrupter during summer conditions when opened and to act as a solid boundary layer during winter conditions when closed. Even though this is a good design to keep the heat from reaching the house, it is impractical as the cost of materials needed would increase.

References

1. Hyun, J. M. (1994). Unsteady buoyant convection in an enclosure. *Advances in Heat Transfer*, 24, 277–320.
2. Ostrach, S. (1988). Natural convection in enclosures. *Transactions of the ASME: Journal of Heat Transfer*, 110, 1175–1190.
3. Markatos, N. C., & Pericleous, K. A. (1984). Laminar and turbulent natural convection in an enclosed cavity. *International Journal of Heat and Mass Transfer*, 27(5), 755–772.
4. Bejan, A. (2013). *Convection heat transfer*. Hoboken: Wiley.
5. Saha, S. C., & Khan, M. M. K. (2011). A review of natural convection and heat transfer in attic-shaped space. *Energy Building*, 43, 2564–2571.
6. Probert, S. D., & Thirst, T. J. (1977). Thermal insulation provided by triangular sectioned attic spaces. *Applied Energy*, 3, 41–50.
7. Thirst, T. J., & Probert, S. D. (1978). Heat transfer versus pitch angle for nonventilated triangular-sectioned, apex-upward air-filled spaces. *ASTM Special Technical Publication*, 660, 203–210.
8. Flack, R. D. (1980). The experimental measurement of natural convection heat transfer in triangular enclosures heated or cooled from below. *Transactions of the ASME: Journal of Heat Transfer*, 102, 770–772.

9. Flack, R. D. (1979). Velocity measurements in two natural convection air flows using a laser velocimeter. *Transactions of the ASME: Journal of Heat Transfer*, 101, 256–260.
10. Poulidakos, D., & Bejan, A. (1983). Natural convection experiments in a triangular space. *Journal of Heat Transfer*, 105, 652–655.
11. Poulidakos, D., & Bejan, A. (1983). The fluid dynamics of an attic space. *Journal of Fluid Mechanics*, 131, 251–269.
12. Ridouane, E. H., Campo, A., & McGarry, M. (2005). Numerical computation of buoyant airflows confined to attic spaces under opposing hot and cold wall conditions. *International Journal of Thermal Sciences*, 44, 944–952.
13. Ridouane, E. H., Campo, A., & Hasnaoui, M. (2006). Benefits derivable from connecting the bottom and top walls of attic enclosures with insulated vertical side walls. *Numerical Heat Transfer, Part A—Applications*, 49, 175–193.
14. Salmun, H. (1995). The stability of a single-cell steady-state solution in a triangular enclosure. *International Journal of Heat and Mass Transfer*, 18, 363–369.
15. Farrow, D. E., & Patterson, J. C. (1993). On the response of a reservoir sidearm to diurnal heating and cooling. *Journal of Fluid Mechanics*, 246, 143–161.
16. Asan, H., & Namli, L. (2002). Numerical simulation of buoyant flow in a roof of triangular cross-section under winter day boundary conditions. *Energy Buildings*, 33, 753–757.
17. Asan, H., & Namli, L. (2000). Laminar natural convection in a pitched roof of triangular cross-section: Summer day boundary conditions. *Energy Buildings*, 33, 69–73.
18. Holtzman, G. A., Hill, R. W., & Ball, K. S. (2000). Laminar natural convection in isosceles triangular enclosures heated from below and symmetrically cooled from above. *Journal of Heat Transfer*, 122, 485–491.
19. Ridouane, E. H., & Campo, A. (2006). Formation of a pitchfork bifurcation in thermal convection flow inside an isosceles triangular cavity. *Physics of Fluids*, 18, 074102.
20. Saha, S. C., Patterson, J. C., & Lei, C. (2010). Natural convection and heat transfer in attics subject to periodic thermal forcing. *International Journal of Thermal Sciences*, 49, 1899–1910.
21. Saha, S. C. (2011). Unsteady natural convection in a triangular enclosure under isothermal heating. *Energy Buildings*, 43, 701–709.
22. Saha, S. C. (2011). Scaling of free convection heat transfer in a triangular cavity for $Pr > 1$. *Energy and Buildings*, 43(10), 2908–2917.
23. Saha, S. C., Patterson, J. C., & Lei, C. (2010). Natural convection in attics subject to instantaneous and ramp cooling boundary conditions. *Energy Buildings*, 42, 1192–1204.
24. Saha, S. C., Patterson, J. C., & Lei, C. (2010). Natural convection in attic-shaped spaces subject to sudden and ramp heating boundary conditions. *Heat Mass Transfer*, 46, 621–638.
25. Varol, Y., & OZtop, H. F. (2009). Control of buoyancy-induced temperature and flow fields with an embedded adiabatic thin plate in porous triangular cavities. *Applied Thermal Engineering*, 29, 558–556.
26. Varol, Y., & OZtop, H. F. (2007). Natural convection in porous triangular enclosures with a solid adiabatic fin attached to the horizontal wall. *International Communications in Heat and Mass Transfer*, 34, 19–27.
27. Chamkha, A. J. (2010). Double-diffusive natural convection in inclined finned triangular porous enclosures in the presence of heat generation/absorption effects. *Heat and Mass Transfer*, 46(7), 757–768.
28. Anderson, T. (2009). Convection suppression in a triangular-shaped enclosure. *Computational Thermal Sciences*, 1, 121–309.
29. Ridouane, E. H., & Campo, A. (2007). Effects of attaching baffles onto the inclined walls of attic frames for purposes of energy conservation. *Heat Transfer Engineering*, 28, 1–103.
30. Ostrach, S. (1964). Laminar flows with body forces. In Moore, F. K. (Ed.), *Theory of laminar flows*. Princeton: Princeton University Press.
31. Batchelor, G. K. (1954). Heat transfer by free convection across a closed cavity between vertical boundaries at different temperature. *Quarterly of Applied Mathematics*, 12, 209–233.

32. Saha, S. C., Patterson, J. C., & Lei, C. (2011). Scaling of natural convection of an inclined flat plate: Sudden cooling condition. *Journal of Heat Transfer*, 133(4), 041503.
33. Saha, S. C., Gu, Y. T., & Khan, M. M. K. (2015). A natural convection heat transfer in the partitioned attic space. In M. M. K. Khan, & N. M. S. Hassan (Eds.), *Thermo fluids modeling for energy efficiency applications* (1st ed., pp. 59–72). Elsevier (Chapter 3). ISBN-13: 978-0128023976, ISBN-10: 012802397X.